

# Rock weathering creates oases of life in a High Arctic desert

Sara Borin,<sup>1</sup> Stefano Ventura,<sup>2</sup> Fulvia Tambone,<sup>3</sup> Francesca Mapelli,<sup>1</sup> Florence Schubotz,<sup>4</sup> Lorenzo Brusetti,<sup>1†</sup> Barbara Scaglia,<sup>3</sup> Luigi P. D'Acqui,<sup>2</sup> Bjørn Solheim,<sup>5</sup> Silvia Turicchia,<sup>2</sup> Ramona Marasco,<sup>1</sup> Kai-Uwe Hinrichs,<sup>4</sup> Franco Baldi,<sup>6</sup> Fabrizio Adani<sup>3</sup> and Daniele Daffonchio<sup>1\*</sup>

<sup>1</sup>Department of Food Science and Microbiology, University of Milan, I-20133 Milan, Italy.

<sup>2</sup>Istituto of Ecosystem Study, CNR, I-50019 Sesto Fiorentino, Italy.

<sup>3</sup>Department of Crop Science, University of Milan, I-20133 Milan, Italy.

<sup>4</sup>Department of Geosciences, University of Bremen, D-28359 Bremen, Germany.

<sup>5</sup>Department of Biology, University of Tromsø, N-9037 Tromsø, Norway.

<sup>6</sup>Department of Environmental Sciences, University of Venice 'Ca' Foscari', I-30121 Venice, Italy.

## Summary

**During primary colonization of rock substrates by plants, mineral weathering is strongly accelerated under plant roots, but little is known on how it affects soil ecosystem development before plant establishment. Here we show that rock mineral weathering mediated by chemolithoautotrophic bacteria is associated to plant community formation in sites recently released by permanent glacier ice cover in the Midtre Lovénbreen glacier moraine (78°53'N), Svalbard. Increased soil fertility fosters growth of prokaryotes and plants at the boundary between sites of intense bacterial mediated chemolithotrophic iron-sulfur oxidation and pH decrease, and the common moraine substrate where carbon and nitrogen are fixed by cyanobacteria. Microbial iron oxidizing activity determines acidity and corresponding fertility gradients, where water retention, cation exchange capacity and nutrient availability are increased. This fertilization is enabled by abundant mineral nutrients and reduced forms of iron and sulfur in pyrite minerals within a**

**conglomerate type of moraine rock. Such an interaction between microorganisms and moraine minerals determines a peculiar, not yet described model for soil genesis and plant ecosystem formation with potential past and present analogues in other harsh environments with similar geochemical settings.**

## Introduction

The factors affecting initial steps of soil formation, ecosystem development and plant establishment in extreme arid environments like cold and hot deserts, where the availability of water and nutrients limits biomass growth (Sundareshwar *et al.*, 2003; Yoshitake *et al.*, 2007), are poorly constrained. In arid systems, organismic responses result from overcoming a threshold in water availability, which is key limiting factor (Ogle and Reynolds, 2004; Schwinning *et al.*, 2004; López *et al.*, 2008). Such responses may trigger dramatic changes and, after a cascade of events, finally manifest in comparably immense increases of biomass in soil in conjunction with increase in biological diversity and profound changes in the landscape. Such a behaviour holds also true for microbial life, which include true primary colonizers either autotrophic like photosynthetic cyanobacteria, or heterotrophic microorganisms (Hodkinson *et al.*, 2002). For instance in biological soil crusts, certain cyanobacteria quickly respond to water inputs and move actively towards the moist soil surface or refuge in the deeper soil layers when soil undergoes drying conditions (García-Pichel and Pringault, 2005).

Mineral weathering in soil enhances availability of water and nutrients, leading to an increase of fertility (Anderson *et al.*, 2000; Bashan *et al.*, 2002; Puente *et al.*, 2004a,b; Konhauser, 2007; Yoshitake *et al.*, 2007). Weathering occurs in hot and cold deserts (Ascaso *et al.*, 1990; Adams *et al.*, 1992). During primary colonization of rock substrates, mineral weathering is strongly accelerated under plant roots (Bashan *et al.*, 2002; Uroz *et al.*, 2007) and enhanced by the association with rhizoplane microbiota (Carrillo-García *et al.*, 1999; Bashan *et al.*, 2000), but little is known on how weathering affects the soil ecosystem development before plant establishment.

Arctic glacier moraines recently released from permanent ice cover are ideal models for the assessment of factors associated with the initial development of a mature

Received 20 March, 2009; accepted 11 August, 2009. \*For correspondence. E-mail danielle.daffonchio@unimi.it; Tel. (+39) 250319117; Fax (+39) 250319238. †Present address: Faculty of Science and Technology, Free University of Bozen/Bolzano, Via Sernesi 1, 39100 Bolzano, Italy.

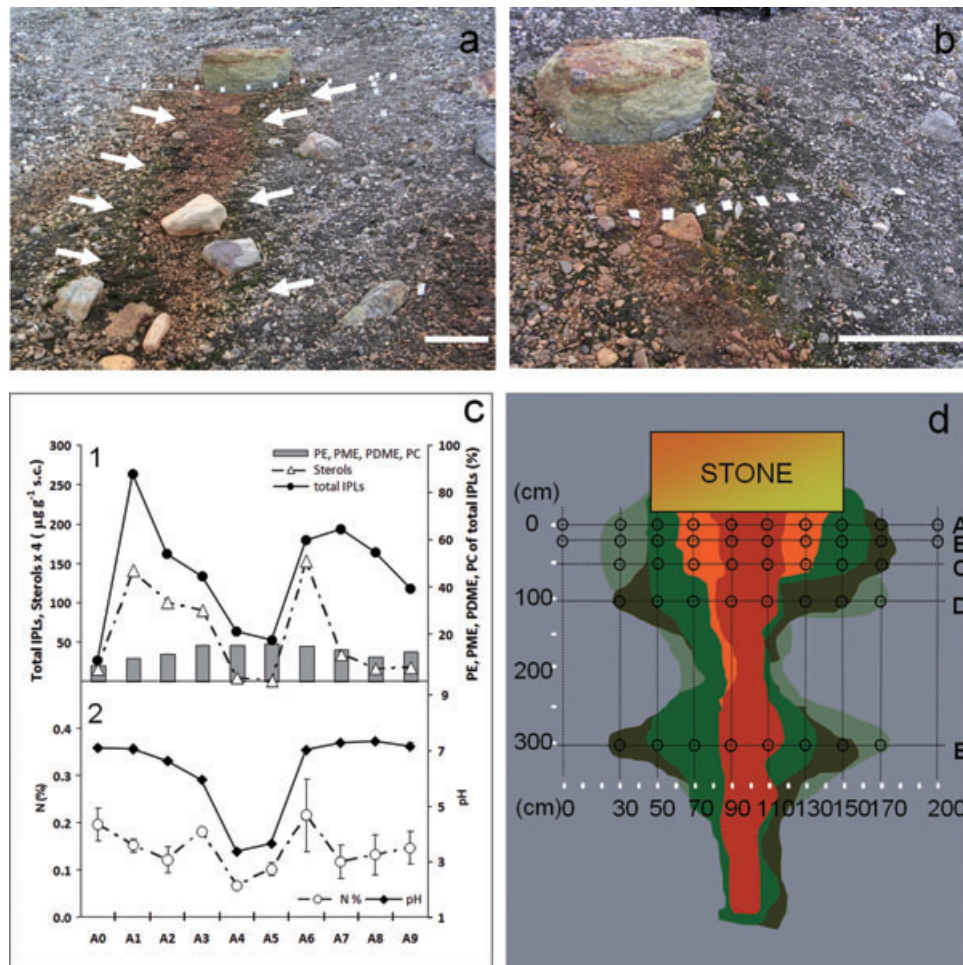


**Fig. 1.** The ML-RS1 site in the moraine of Midtre Lovénbreen glacier, Ny Ålesund, Svalbard.

A. A rusty leaching strip departs from a stone within the grey-coloured moraine (white bar = 50 cm). White arrows indicate zones where dense plant biomass can be observed. A detail of an area densely colonized by plants within the site is shown in (B) (white bar = 50 cm).

C. Biological markers measured along transect A, located 5 cm underneath the stone. C1, Absolute abundances of total IPLs and sterols along transect A and the relative contribution of phosphatidylethanolamine (PE), phosphatidyl-(N)-methylethanolamine (PME) and phosphatidyl-(N,N)-dimethylethanolamine to total IPLs. C2, percentage of nitrogen and pH values in the soil crust.

D. Map of the area showing the position of the sampling transects.

soil ecosystem. Within the grey-coloured moraine of the Midtre Lovénbreen glacier (78°53'N), Svalbard, between the Hodkinson proglacial chronosequence sites ML2 and ML3, which were released from the permanent ice cover 23 and 44 years ago respectively (Hodkinson *et al.*, 2003), we found several sites densely colonized by the mosses *Ditricum flexicaule* and *Bryum* sp. and the vascular plant *Saxifraga oppositifolia* (Hodkinson *et al.*, 2003) (Fig. 1A and B). Green strips of flourishing vegetation were adjacent to rusty iron oxide-leaching strips sloping along the moraine with the latter departing from yellowish-rusty-greenish stones, rock conglomerates rich in reduced iron, in the form of pyrite. In a defined area of the moraine we found several of these rusty and green strips that were exclusively associated with one particular stone type.

Here, we present evidence that under harsh conditions of recently deglaciated moraines of the High Arctic, enhanced rock weathering mediated by chemolithoautotrophic bacteria is associated to soil formation and increases of soil fertility that fosters the early establishment and growth of plant biocoenosis, the ecological community of plants that sustains the ecosystem.

## Results and discussion

We initially focused on one of these sites, named ML-RS1, estimated to be released by ice about 27 years ago. We observed several sites like ML-RS1 in the south-east portion of the moraine. We counted at least four sites similar to ML-RS1 with stones of similar size. In an area of about 1 hectare of the moraine we observed tens of smaller

sites with much smaller stones where signs of the plant flourishing like those in site ML-RS1 were present. We also found a larger site named ML-RC1 with the same but more extended phenomenon in place (Fig. S1). Plant flourishing occurred where the type of conglomerate rock like that of site ML-RS1 emerged to open air from the subsurface. For instance, site ML-RC1 looked like a large conglomerate vein cropping out from the grey moraine.

X-ray diffractometry and scanning electron microscopy-energy dispersive X-ray analyses of thin sections of the stone at site ML-RS1 showed pyrite microcrystals (Fig. 2). The stone was a conglomerate consisting mainly of quartz, cemented by kaolinite, with additional contributions of pyrite, aluminium-silicates, calcium hydroxyapatite and manganese oxides. On the surface, besides jarosite and gypsum, iron oxy-hydroxides and oxides could be detected as well as small amounts of organic carbon (0.3% w/w), supporting the presence of microbial biomass.

A higher density of plants was apparent in the green strip of site ML-RS1 compared with the surrounding greyish moraine. Plant and/or eukaryotic algal sterols, dominated by campesterol and sitosterol, were 10–100 times more concentrated in the green strips than in the surrounding moraine. The sterol concentrations declined to values close to zero in the rusty strip, suggestive of hostile conditions for plants and eukaryotic microorganisms (Fig. 1C1). Intact polar lipids (IPLs), representative of viable cells (Sturt *et al.*, 2004; Biddle *et al.*, 2006; Lipp *et al.*, 2008), showed a similar pattern as the sterols, with highest concentrations in the green strips and lower values in the rusty and moraine areas. The sharp decline of sterols in the rusty area suggests that the IPLs in this zone largely represent bacterial biomass.

The composition of IPLs in the transect was diverse and represented a mixture of eukaryotic and bacterial biomass, largely derived from phototrophic organisms. Abundant IPLs were betaine lipids linked to mono- and polyunsaturated fatty acids, glycolipids esterified to polyunsaturated fatty acids and phosphoglycerolipids with saturated and monounsaturated fatty acids (see Supporting information, Table S1, Fig. S4). This combination of lipids is typical of lower plants and arctic mosses (Dembitsky and Řezanka, 1995), cyanobacteria (Řezanka *et al.*, 2003) and bacteria involved in plant symbiosis (López-Lara *et al.*, 2003). Heterocyst glycolipids from nitrogen-fixing cyanobacteria (Nichols and Wood, 1968) were detected in high amounts throughout the transect (~20% of total IPLs), indicating that heterocyst cyanobacteria are evenly distributed in the green and rusty area (see Supporting information, Fig. S4). Towards the rusty strip, the phospholipids phosphocholine (PC), phosphoethanolamine (PE),

phospho-(N)-methylethanolamine (PME) and phospho-(N,N)-dimethylethanolamine (PDME) increase (Fig. 1C1). These lipids are commonly observed in cultures of acidophilic bacteria, e.g. *Acidithiobacillus ferrooxidans* and *Acidiphilium* (Barridge and Shively, 1968; Harms, 2007), and thus are consistent with an increase of these bacteria in the rusty strip. Ornithine lipids and bacteriohopanepolyols bacteriohopane-32,33,34,35-tetrol and 35-aminobacteriohopane-32,33,34-triol (aminotriol), which are exclusive bacterial markers (Lopez-Lara *et al.*, 2003; Talbot *et al.*, 2008), were also detected in low abundances throughout the transect, however, with highest amounts outside the rusty area. We assign the presence of these lipids to bacteria associated with plant-symbiosis of the order *Rhizobiales*, which were detected in the green area (Fig. 3, Table S4). In summary, the elevated biomass content adjacent to the rusty strip underscores the link between increased fertility by rock weathering and the establishment of an oasis of life.

To examine microenvironmental conditions promoting plant growth, we established a grid pattern for a detailed sampling of site ML-RS1 (Fig. 1D) along mini-transects at increasing distance from the stone. Total organic carbon, nitrogen percentage, potential nitrogen fixation and respiratory activity were higher in the green than in the rusty strip, but similar to those in the surrounding greyish moraine (Fig. 1C2, Table S2). Stable isotopic compositions of nitrogen  $\delta^{15}\text{N}$ , of slightly below 0‰ indicated that in all transects bacterial nitrogen fixation is the main source of nitrogen (Högberg, 1997). The presence of heterocyst glycolipids in all samples (Fig. S4) strongly supports this interpretation. We conclude that nitrogen supply is provided to both the green and the greyish soil crusts and is probably not limiting plant growth in the green strip.

We determined parameters indicative of soil fertility in the grid pattern of site ML-RS1 after removal of the plant cover (Table S2). Mean values of fine particles, cation exchange capacity (CEC), water holding capacity (WHC), exchangeable Mg, K and Fe and  $\text{Fe}^{2+}$  were significantly higher in the green than in the greyish crusts. Relative increments, for the whole soil crust (Table 1), were between 36.2% ( $K_{\text{exch}}$ ) and 132% ( $\text{Fe}_{\text{exch}}$ ), with CEC and WHC, respectively, increasing of 95.2% and 48.1%. Nutrient differences are particularly meaningful considering that in the green strip plants act as element scavengers and bioaccumulators that continuously extract nutrients from the soil crust. The increased WHC markedly supports more favourable conditions for plant growth in this desert ecosystem that receives an average precipitation of 190 mm year<sup>-1</sup> (range, 88–265 mm in the period 1988–2002; <http://www.svalbard.com/weather.html>). Such low values indicate that water is the primary limiting factor for development of plant biocoenoses (Ogle and Reynolds, 2004; Lopez *et al.*, 2008).

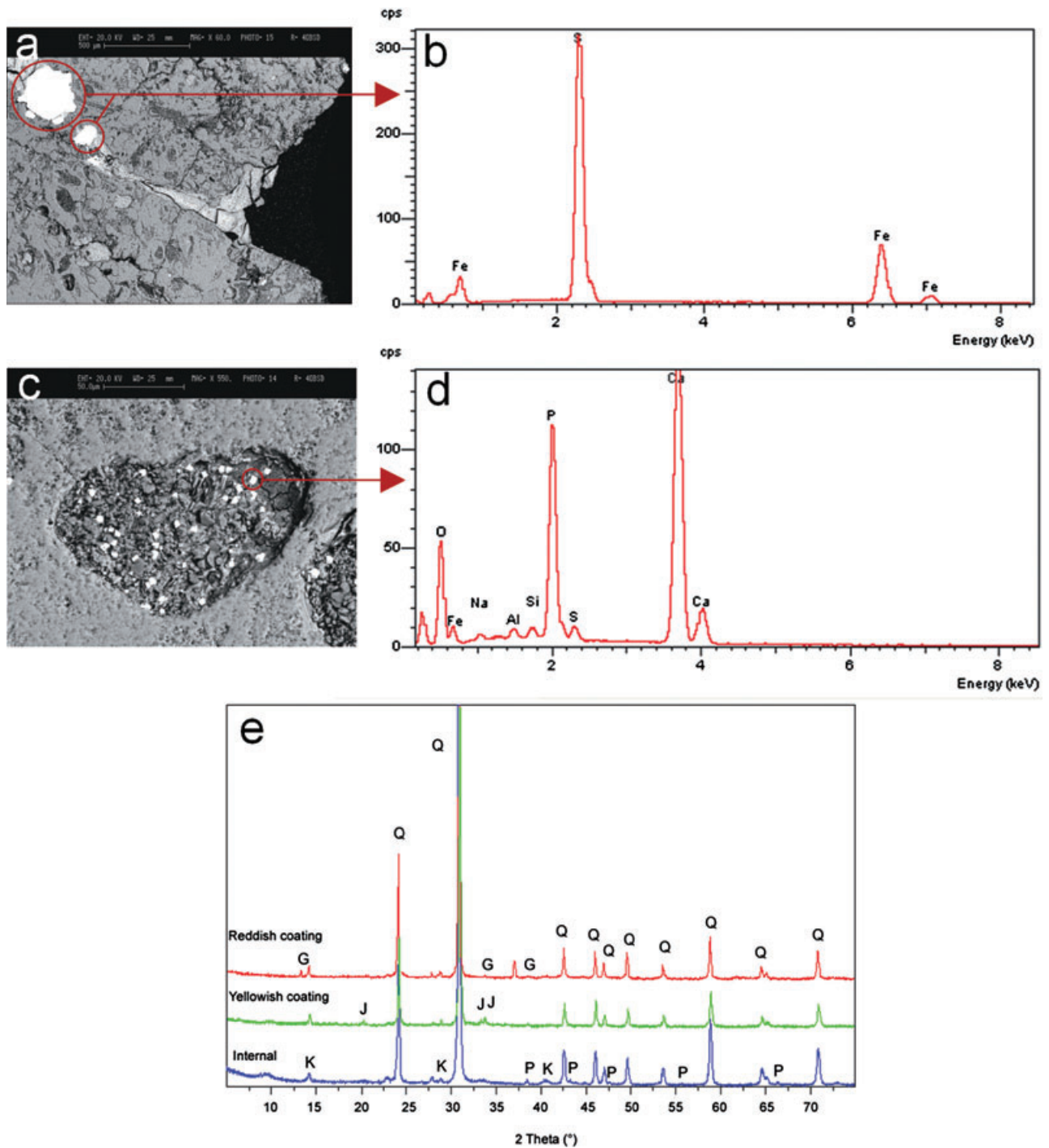


**Fig. 2.** Pyrite microcrystals and oxidation signatures on the surface of the stone upstream the rusty strip of site ML-RS1. A and C. SEM-EDX back scattering electron micrographs of thin-layer shiny sections of the stone, showing pyrite and apatite microcrystals (circled) respectively. Peaks attributable to the different elements of pyrite and apatite crystals, circled in (A) and (C), are shown in (B) and (D) respectively. E. X-ray diffractograms of the surface and the internal part of the conglomerate. Diffractograms of the yellowish and rusty coatings and the internal part of the stone are shown in red, green and blue colours respectively. Marked peaks are G, gypsum; J, jarosite; K, kaolinite; P, pyrite; Q, quartz.

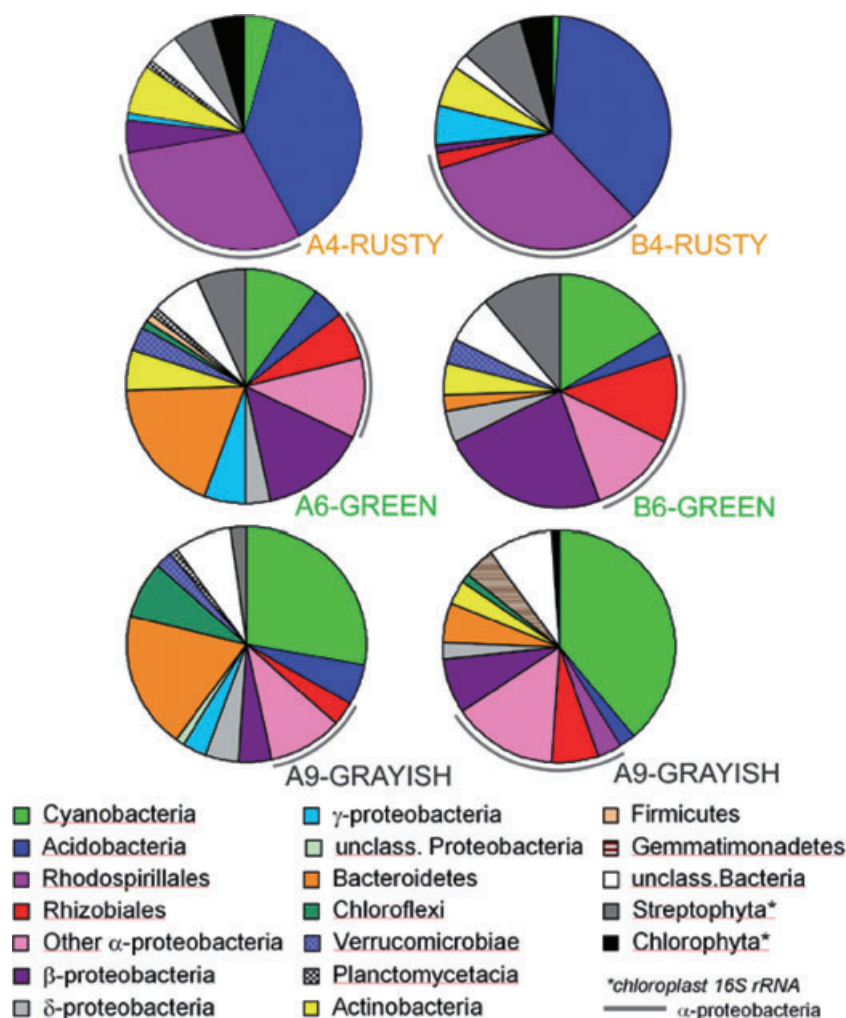


**Fig. 3.** Bacterial diversity in the soil crusts of site ML-RS1 in the moraine of Midtre Lovénbreen glacier, Ny Ålesund, Svalbard. Each graph shows the relative composition of the bacterial community inhabiting the soil crust. A4 and B4 were samples from the rusty soil crust, A6 and B6 from the green soil crusts and A9 and B9 from the greyish soil crusts. Ninety clones have been randomly sequenced from each library. Sequencing primer started from position 27 and the sequence length was 700–900 bp.

A low pH was measured (Fig. 1C, Table S2) in the rusty strip (down to 3.5; mean value along the rusty vertical transect,  $5.2 \pm 1.4$ ,  $n=10$ ) and presented a raising gradient in the green strips ( $7.1 \pm 0.3$ ,  $n=25$ ) to reach neutral-subalkaline values in the greyish moraine ( $7.6 \pm 0.4$ ,  $n=9$ ). pH is significantly correlated with both

total ( $Fe_{tot}$ ) and exchangeable ( $Fe_{exch}$ ) iron contents ( $r=-0.959$ ,  $P<0.01$ ,  $n=15$ , and  $r=-0.932$ ,  $P<0.01$ ,  $n=15$  respectively). We hypothesized that ferrous iron, present in the form of pyrite, was dissolved and transported from the conglomerate stone, and subsequently oxidized to form the acidic rusty strip.  $Fe^{2+}$  oxidation was

**Table 1.** Parameters indicative of soil fertility in the greyish and green soil crusts of site ML-RS1 and relative percentage increments in the green respect to the greyish crusts over the whole soil crust (fine plus coarse particle fractions).

| Parameters                                    | Soil crust type <sup>a</sup> |              | Relative increment <sup>b</sup><br>(%) |
|-----------------------------------------------|------------------------------|--------------|----------------------------------------|
|                                               | Greyish                      | Green        |                                        |
| CEC (cmol <sup>(+)</sup> kg <sup>-1</sup> dm) | 2.9 ± 0.9                    | 5.7 ± 1.5    | 95.2                                   |
| WHC (g 100 g <sup>-1</sup> dm)                | 21.6 ± 2.9                   | 32.0 ± 8.7   | 48.1                                   |
| $Fe_{exch}$ (mg kg <sup>-1</sup> dm)          | 65.4 ± 27.8                  | 151.8 ± 28.5 | 132.0                                  |
| $Fe^{2+}$ (mg kg <sup>-1</sup> dm)            | 34.2 ± 6.2                   | 50.0 ± 5.4   | 46.4                                   |
| $Mg_{exch}$ (mg kg <sup>-1</sup> dm)          | 73.4 ± 20.4                  | 113.6 ± 15.8 | 54.7                                   |
| $K_{exch}$ (mg kg <sup>-1</sup> dm)           | 103.2 ± 29.0                 | 140.8 ± 35.1 | 36.2                                   |

a. All means are significantly different ( $P<0.05$ ) according to Duncan test.

b. Relative percentage increments of parameters in the green crust respect to the greyish crust. exch, exchangeable.

corroborated by the lower  $\text{Fe}^{2+}$  content in the rusty than in the green strips, despite  $\text{Fe}_{\text{tot}}$  and  $\text{Fe}_{\text{exch}}$  contents were significantly higher (Table S2). The hypothesis is consistent with the presence of jarosite [ $\text{KFe}_3(\text{SO}_4)_2(\text{OH})_6$ ] on the stone surface and within the rusty strip as shown by Diffuse Reflectance Infrared Fourier Transformed (DRIFT) spectroscopy (Fig. S2A). Jarosite has been used as a water signature on Mars (Klingelhofer *et al.*, 2004), but is unstable and rare under oxic conditions on Earth (Darmody *et al.*, 2007). Jarosite can be formed by spontaneous or microbially mediated oxidation of pyrite (Sasaki and Konno, 2000). The evidence at site ML-RS1 is consistent with such a scenario.

The observed physicochemical differences between the rusty, green and greyish strips are reflected in the structures of the respective bacterial communities. Bacterial diversity was higher in the green and the greyish than in the rusty strips that appeared as the least equitable as shown by Shannon–Wiener and Equitability indices of bacterial amplified ribosomal intergenic spacer analysis (ARISA) (Table S3). Detrended correspondence analysis of ARISA profiles tended to cluster the samples according to the soil crust pH, indicating that different bacterial communities were present in the different soil crusts (Fig. S3). Soil crust pH was strongly correlated with bacterial diversity (ARISA detrended correspondence analysis axis 1 versus pH,  $r = 0.835$ ,  $P < 0.001$ , Fig. S3). Soil pH has already been shown as a major driver of biogeographical repartition of bacteria in soil (Fierer and Jackson, 2006). To identify bacteria inhabiting the soil crusts, clone libraries of amplified 16S rRNA genes were generated from six soil crust samples within the grid pattern, two for each colour (rusty, greenish and greyish strips) in two horizontal transects sampled at 5 and 23 cm from the stone originating the leaching strips. A total of 540 clones were sequenced (Fig. 3, Table S4). The rusty soil crusts were dominated by  $\alpha$ -*Proteobacteria* of the genus *Acidiphilium* (order *Rhodospirillales*; 30–32% of the clones in the two libraries respectively) and by *Acidobacteria* (37–39% of the clones respectively), both frequently associated to acidic environments where oxidation of iron and sulfur occur (González-Toril *et al.*, 2003; Diaby *et al.*, 2007). The greyish soil crusts were dominated by *Cyanobacteria* (29–40% of the clones respectively) followed by  $\alpha$ -*Proteobacteria* mostly affiliated with orders other than *Rhodospirillales*. In contrast, green soil crusts showed a bacterial community typical of plant-inhabited soils. Hence, at the boundary between a cyanobacterial carpet typical of substrates recently released by permanent ice cover (Nemergut *et al.*, 2007), and iron weathering spots, the geochemical conditions selected a rhizosphere-like bacterial community able to support a plant biocoenosis. We suggest that the major driver of

such community transition was the pH gradient resulting from the activity of iron-oxidizing bacteria.

By inoculating an organic carbon-free medium added with reduced iron sulfate either with the stone surface or the rusty soil crust, we isolated rod-shaped bacteria able to grow at 4°C and pH 2 and to produce jarosite (Fig. S2B). The isolates were identified as *A. ferrooxidans* by 16S rRNA gene sequencing and contained phosphatidyl-(N)-methylethanolamine (94% of total IPLs) as a major lipid type, next to phosphatidylglycerol and ornithine lipids (Fig. S4), all of which are present in the rusty strip and surrounding area. At a second site (ML-RC1) that resembles site ML-RS1 (Fig. S1), *A. ferrooxidans* counts decreased from  $1.7 \times 10^4$  cells  $\text{g}^{-1}$  close to the rock to  $3.0 \times 10^0$  at about 10 m distance from the leaching origin. Using the major lipid PME of *A. ferrooxidans* as a proxy for estimating this organism's contribution to the microbial population, we infer that in ML-RS1 site it accounts not more than 0.8% of the total community in transects A and B (Fig. S4). The mean abundance of the PME derivatives found in *A. ferrooxidans* decreases with distance from the rock, from ~0.4% (transect A) to ~0.2% (transect B) as cell counts decrease. This is consistent with the failure of 16S rRNA gene libraries in detecting this species. *Acidithiobacillus ferrooxidans* gains energy upon iron oxidation, one of the less energy-releasing metabolic processes ( $\Delta G^\circ_r = -27.2$  KJ  $\text{mol}^{-1}$ , pH 2.5 Konhauser, 2007). Taking into account different estimates of *Acidithiobacillus* efficiency in the reaction, it was calculated that it would need to oxidize between 50 and 500 mol of ferrous iron to assimilate one mol of carbon (Ehrlich and Newman, 2008). As a consequence, *A. ferrooxidans* cell abundance can be very low, despite high iron oxidation activity.

In summary, specific sites within the Midtre Lovénbreen moraine, where stones rich in reduced iron and sulfur are present, provide conditions suitable to support growth and activity of an acidophilic iron-oxidizing bacterial community. Progressive stone fracturing and surface desegregation due to winter freezing, and chemical and biological weathering, and the water-mediated particle dragging maintained a constant pyrite supply over time on the substrate slope downstream the stone, allowing the establishment of a chemolithoautotrophic bacterial community (Fig. 4A). Stone leaching during summer snow melting created a gradient along the slope with decreasing iron concentration and acidification, as shown by the increasing pH along the rusty strip (Table S2). Oxidation of reduced iron released from the stone caused jarosite and ferric oxy-hydroxide formation responsible for the increase of both soil crust specific surface area (SSA) and CEC, the latter determining a higher WHC and nutrient content in the green strip (Table 1; Fig. 4B). The positive and negative correlations between SSA and total and

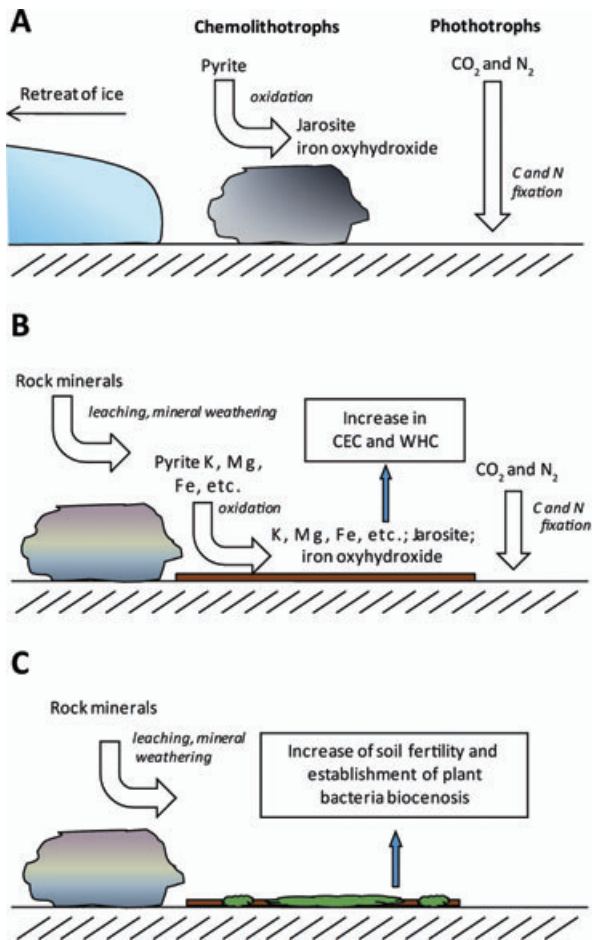


Fig. 4. A schematic of the overall process occurring in ML-RC1 site in the moraine of the Midtre Lovénbreen glacier, Svalbard.

reduced iron contents, respectively,  $r = 0.835$ ,  $P < 0.0001$  ( $n = 15$ ) and  $r = -0.599$ ,  $P < 0.01$  ( $n = 15$ ), supported such a mechanism. Hence, with respect to the rest of the moraine, plant establishment was favoured by the combination of increased soil crust fertility (Fig. 4C) driven by the acidification and leaching activity of a chemolithotrophic community strongly influenced by iron oxydizers, and by cyanobacteria-mediated primary productivity.

The synergy between these two bacterial autotrophic processes in favouring microorganism and plant colonization is probably not restricted to the Midtre Lovénbreen glacier foreland, but should be explored in other environments where similar geochemical conditions exist (Anderson *et al.*, 2000; Skidmore *et al.*, 2005; Darmody *et al.*, 2007), such as natural pyritic belts (Fernández-Remolar *et al.*, 2005) and manmade pyritic mine tailings (Southam and Beveridge, 1992). Such a synergy could also have played a role in the primordial land colonization by plants (Rensing *et al.*, 2008) or in soil formation on extraterrestrial bodies where signatures of acidic aqueous systems with iron- and sulfur-based redox cycles have been found (Bibring *et al.*, 2007).

### Establishment of early successional communities

**Trigger mechanism:** Retreat of ice.

**Consequences:** Rock and soil colonisation by (1) chemolithotrophs (*Acidithiobacillus*) mediating sulfur and iron oxidation, and (2) photoautotrophs (*Cyanobacteria*) mediating carbon and nitrogen fixation.

**Implications:** (1) Oxidation of rock mineral pyrite to iron precipitates, i.e. jarosite and iron hydroxides (2) accumulation of C and N in soil.

### Establishment of pH gradient and soil fertility

**Trigger mechanism:** Protracted leaching of rock minerals by winter freezing/summer thawing and water-mediated particle dragging.

**Consequences:** Continuous oxidation of ferrous iron to iron oxyhydroxides, determining a gradient with low pH in the rusty area.

**Implications:** (1) Oxyhydroxides increase specific surface area (SSA), cation exchange capacity (CEC) and consequently water holding capacity (WHC), (2) low pH enhance nutrient solubilization.

### Establishment of plant rhizosphere

**Trigger mechanism:** Fertility improvement by: (1) WHC increase, (2) CEC increase and nutrient availability enhancement, and (3) improvement of soil structure by C and N fixed by *Cyanobacteria*.

**Consequences:** Higher fertility determines an advancement of soil formation that allows heterotrophic bacteria proliferating and plant establishing.

**Implications:** (1) Formation of a stable rhizosphere bacterial community. (2) Establishment of a bacteria-plant biocenosis.

### Experimental procedures

Soil crusts in the moraine of the Midtre Lovénbreen glacier, Ny Ålesund, Svalbard, were collected during three expeditions in August 2004 and 2005 and early September 2006 within the sampling grid designed on site ML-RS1 (Midtre Lovénbreen Rusty Site 1; 78°53.753'N, 12°05.115'E; 57.1 m a.s.l.) and along the slope of site ML-RC1. The top 5 mm of the crusts were separated from the underlying mineral matter and the two fractions were separately processed. Recovered samples were stored at  $-20^{\circ}\text{C}$  for chemical and nucleic acid-based studies, or at  $4^{\circ}\text{C}$  for microbiological enrichments or activity measurements.

#### Soil crust and stone chemical analysis

Soil parameters were determined as follows: soil crusts pH in aqueous solution using a 1:2.5 sample/water ratio; fine ( $< 2$  mm) and coarse ( $> 2$  mm) particles by soil sieving after drying; total nitrogen by Kjeldahl method; available-P by using the Olsen and Bray and Kurtz methods depending on the pH; organic carbon by wet oxidation. For CEC and exchangeable Ca, Mg, K, Na determinations, samples were saturated with  $\text{BaCl}_2$ -Triethanolamine solution (pH 8.1) and exchangeable cations were determined by Inductively

Coupled Plasma (ICP-MAS VARIAN, Liberty AX, Walnut Creek, CA). Total Ca, Mg, K, Na, Fe and Al were determined by samples digestion with  $\text{HNO}_3$  ( $16 \text{ mol l}^{-1}$ ) in a microwave furnace (CEM Mars 5, Matthevs, North Caroline), and successive detection by Inductively Coupled Plasma. All the above methods were as described in Pansu and Gautheyrou (2006). WHC was determined by the Stackman box method (Klute, 1986). Exchangeable iron forms were extracted with EDTA or DTPA depending on crust pH (Lindsay and Norwell, 1969; Lakanen and Erviö, 1971) and determined with an Inductively Coupled Plasma. Reduced iron forms were extracted with the coloured EDTA-BPDS solution and quantified spectrophotometrically at 535 nm (Wang and Peverly, 1998). SSA of soil crust samples were determined by  $\text{N}_2$  adsorption (BET method) of dried samples by using a sorptometer apparatus (Quantachrome NovaWin2, NOVA Instruments, Boynton Beach, FL, USA). All analytical data were determined on the fine particle fraction ( $< 2 \text{ mm}$ ) (Pansu and Gautheyrou, 2006). Parameters with statistically significant differences between the greyish and the green crusts (Table S2) were also referred to the whole sample (Table 1) by taking into account the fine and the coarse particle contents of the whole soil crust and their standard deviations recalculated according to statistical standards (Ciani *et al.*, 1990). All the analyses were made in triplicate and the results were analysed by ANOVA, considering the colour strips as independent variables. Values of the means were separated by Duncan test, considering a significance level of  $P < 0.05$ . All statistical analyses were performed using the SPSS 13.0 software package (SPSS International, Chicago, IL, USA).

Stable nitrogen isotopes were determined from 20 to 30 mg of homogenized soil on an elemental analyser (ThermoQuest EA/NA 1110) coupled to a Thermo Finnigan Delta Plus isotope ratio mass spectrometer via a ConFlow II interface. Analyses were calibrated with a known standard (Wadden Sea soil) and were normalized to the international standard IAEA-CH-6, sucrose.

Shine thin sections of stone samples for Environmental Scanning Electron Microscopy-Energy Dispersive X-ray spectroscopy were visualized by a scanning electron microscope (FEI Quanta mod. 200, Endhoven, NI) at an acceleration voltage of 25 kV to determine elements in soil particles (triplicate) at 1.0 and 0.1 bar after 100 s scanning. Mean concentrations and standard deviations of each element were calculated from three random determinations at different spots on the samples. The X-ray beam was  $4 \mu\text{m}$  wide and penetrated to a depth of  $2 \mu\text{m}$ .

X-ray diffractometry was performed on samples collected from the surface of the conglomerate on the basis of the different coating colours, reddish and yellowish, and from the internal part of the rock. Due to the rock nature, it was easy to break and separate the first 2–3 mm of the rock. Powdered samples were analysed by a Philips PW 3830 X-ray diffractometer using  $\text{CoK}\alpha$  radiation incident from  $3$  to  $75^\circ\theta$  with a step size of  $0.02^\circ\theta$  and a scan step time of 1 s. Total C and N content were determined using a Carlo Erba (Milan, Italy) NA 1500 CHNS Analyser. To distinguish organic from inorganic C was used a procedure reported in Santi and colleagues (2006). Two aliquots of each sample, in two replicates, were analysed by dry combustion: the first without treatment, to assess the total C and N content and the other after treatment

with excess HCl, for carbonate removal, to assess only the organic C content.

Rock samples and jarosite were analysed by DRIFT spectroscopy using an Avatar 370 FT-IR from ThermoNicolet Instruments (Madison, WI, USA). Samples previously dried at  $65^\circ\text{C}$  for 48 h, and KBr (FT grade, Aldrich Chemical Co, ST Louis, Missouri) were mixed in the 1:10 ratio (w/w) and finely ground for 10 min using an agate ball mill (Specamill-Greeseby-Specac, Kent, UK). Instrument parameters used were: scanning 128, resolution  $4 \text{ cm}^{-1}$ , and frequency  $400\text{--}4000 \text{ cm}^{-1}$  gain 16. Peaks assignments were made according to Sasaki and Konno (2000).

#### Lipid biomarkers

Lipid analysis followed the procedures outlined by Sturt and colleagues (2004). In brief, 5–10 g of freeze-dried soil was extracted using a modified Bligh and Dyer protocol. Total lipid extracts were analysed on a ThermoFinnigan LCQ Deca XP Plus HPLC-MS system in positive and negative ionization mode. Quantification of IPLs was achieved using an internal standard (1-O-hexadecyl-2-acetyl-sn-glycero-3-phosphocholine) and external calibration of this standard. For the analysis of bacteriohopanepolyols, an aliquot of the total lipid extract was acetylated with acetic anhydride/pyridine (1:1) for 1 h at  $50^\circ\text{C}$  and subsequently measured on the same HPLC system using conditions described by Talbot and colleagues (2008). Sterols were analysed in an alcohol fraction that was isolated by solid-phase extraction and derivatized according to Hinrichs and colleagues (2000). The fractions were measured on a ThermoFinnigan Trace GC coupled to a Finnigan Trace MSplus and to a Finnigan DSQ.

#### Microbial community studies

Total DNA was extracted with the FastDNA SPIN Kit for Soil (BIO 101 Systems Q-BIO gene; CA, USA) following manufacturer's instructions. The ARISA fingerprinting was determined as described elsewhere (Cardinale *et al.*, 2004) and downstream multivariate statistical analyses were done with MVSP software (Kovach Computing Services, UK). 16S rRNA gene clone libraries from selected soil crust samples of site ML-RS1 were prepared as previously described (Van der Wielen *et al.*, 2005). Ninety clones have been randomly chosen from each library. 700- to 900-bp-long sequences, corresponding to the first half of the 16S rRNA gene, were aligned with ClustalX (Thompson *et al.*, 1997), and operational taxonomic unit distribution was calculated with Vector NTI Advance 10 using a 97% identity threshold. Good coverage of the dominant operational taxonomic units within libraries was evaluated by rarefaction analysis with PAST software (Hammer *et al.*, 2001).

#### Isolation and cultivation of chemolithoautotrophs

One gram of rusty soil crusts or stone surface was inoculated in carbon-free 9K medium supplemented with ferrous sulfate (Lizama and Suzuki, 1988) and incubated at  $4^\circ\text{C}$  for 4 weeks until a rusty precipitate of iron oxides was visible, and

bacterial cells were observable. Three subsequent steps of terminal dilution to extinction enabled obtaining pure cultures of rod-shaped bacteria. A 16S rRNA gene library from the culture was established, and the sequencing of several clones revealed identical sequences having 99% identity with the 16S rRNA gene of *A. ferrooxidans*. The isolated strains were cultured in modified 9K (Silverman and Lundgren, 1959) supplemented with either ferrous sulfate or powdered pyrite (0.5% W/V). At 28°C the strains produced jarosite after 3 days of incubation. Most probable number counts of autotrophic iron oxidizing bacteria were performed on soil crusts from site ML-RC1. Soil crusts were inoculated (1% W/V) in decimal serial dilutions in modified 9K medium supplemented with iron (II) sulfate in 3 ml microtiter plates. After 4 weeks of incubation at 15°C growth coincided with the appearance of a rusty precipitate in the wells.

#### Activity measurements

Potential nitrogen fixation activity of soil samples was measured as described elsewhere (Zielke *et al.*, 2002). Freshly collected 1-cm-thick top layer soil crust samples (surface area, 64 cm<sup>2</sup>) were conditioned at room temperature (24°C) in natural light and 0 water potential (water saturated) for 17 h prior to incubation with 10% acetylene (v/v) for 3 h in the same conditions.

Soil crust respirations were measured by trapping with alkali the CO<sub>2</sub> produced during soil crust incubation at 20°C in the laboratory for 21 days (Bekku *et al.*, 1997). All the analyses were performed in triplicate.

#### Acknowledgements

The Authors thank Agostino Rizzi for performing SEM-EDX analysis of thin sections of the stone, Manuela Spagnol for surface area of soil crust samples, Valentina Orzi for respiration activity measurements, Silvia Salati for cation content determinations and Alessandro Dodero for CHNS analysis. Financial support comes from the project FIRST 2007 'Studio della successione microbica lungo un transetto di deglaciazione del ghiacciaio Midtre Lovén, Isole Svalbard (Norvegia)' granted by the University of Milan. S.V. and S.T. acknowledge a travel grant from the ESF Scientific Programme on Nitrogen Fixing Cyanobacteria – CYANOFIX for a 1 month expedition to Svalbard. S.V. acknowledges a short-term mobility grant of CNR to travel to Svalbard. F.S. and K.U.H. acknowledge support by DFG (through MARUM Center for Marine Environmental Sciences) and thank Monika Segl for help during nitrogen isotope analysis. Authors thank CNR-Polarnet for the use of the Italian Polar Station in Ny-Ålesund.

#### References

Adams, J.B., Palmer, F., and Staley, J.T. (1992) Rock weathering in deserts: mobilization and concentration of ferric iron by microorganisms. *Geomicrobiol J* **10**: 99–114.  
 Anderson, S.A., Driver, J.I., Frost, C.D., and Holden, P. (2000) Chemical weathering in the foreland of a retreating glacier. *Geochim Cosmochim Acta* **64**: 1173–1189.  
 Ascaso, C., Sancho, L.G., and Rodriguez Pascual, C. (1990)

The weathering action of saxicolous lichens in maritime Antarctica. *Polar Biol* **11**: 33–40.  
 Barridge, J.K., and Shively, J.M. (1968) Phospholipids of the Thiobacilli. *J Bacteriol* **95**: 2182–2185.  
 Bashan, Y., Davis, E.A., Carrillo-Garcia, A., and Linderman, R.G. (2000) Assessment of VA mycorrhizal inoculum potential in relation to the establishment of cactus seedlings under mesquite nurse-trees in the Sonoran Desert. *Appl Soil Ecol* **14**: 165–175.  
 Bashan, Y., Li, C.Y., Lebsky, V.K., Moreno, M., and de-Bashan, L.E. (2002) Primary colonization of volcanic rocks by plants in arid Baja California, Mexico. *Plant Biol* **4**: 392–402.  
 Bekku, Y., Koizumi, H., Oikawa, T., and Iwaki, H. (1997) Examination of four methods for measuring soil respiration. *Appl Soil Ecol* **5**: 247–254.  
 Bibring, J.-P., Arvidson, R.E., Gendrin, A., Gondet, B., Langevin, Y., Le Mouelic, S., *et al.* (2007) Coupled ferric oxides and sulfates on the martian surface. *Science* **317**: 1206–1210.  
 Biddle, J.F., Fitz-Gibbon, S., Schuster, S.C., Brenchley, J.E., and House, C.H. (2006) Heterotrophic Archaea dominate sedimentary subsurface ecosystems off Peru. *Proc Natl Acad Sci USA* **103**: 3846–3851.  
 Cardinale, M., Brusetti, L., Quatrini, P., Borin, S., Puglia, A.M., Rizzi, A., *et al.* (2004) Comparison of different primer sets for use in automated ribosomal intergenic spacer analysis of complex bacterial communities. *Appl Environ Microbiol* **70**: 6147–6156.  
 Carrillo-Garcia, Á., León de la Luz, J.L., Bashan, Y., and Bethlenfalvay, G.J. (1999) Nurse plants, mycorrhizae, and plant establishment in a disturbed area of the Sonoran Desert. *Restor Ecol* **7**: 321–335.  
 Ciani, G., Fusi, A., Nicotra, F., and Rindone, B. (1990) *Laboratorio di Chimica*. Napoli, Italy: Società Editrice Scientifica.  
 Darmody, R.G., Thorn, C.E., and Dixon, J.C. (2007) Pyrite-enhanced chemical weathering in Kärkevagge, Swedish Lapland. *Geol Soc Am Bull* **119**: 1477–1485.  
 Dembitsky, V.M., and Řezanka, T. (1995) Distribution of diacylglycerylhomoserines, phospholipids and fatty acids in thirteen moss species from southwestern Siberia. *Biochem Syst Ecol* **23**: 71–78.  
 Diaby, N., Dold, B., Pfeifer, H.R., Holliger, C., Johnson, D.B., and Hallberg, K.B. (2007) Microbial communities in a porphyry copper tailings impoundment and their impact on the geochemical dynamics of the mine waste. *Environ Microbiol* **9**: 298–307.  
 Ehrlich, H.L., and Newman, D.K. (2008). *Geomicrobiology*. Florida, USA: CRC Press.  
 Fernández-Remolar, D.C., Morris, R.V., Gruener, J.E., Amils, R., and Knoll, A.H. (2005) The Río Tinto Basin, Spain: mineralogy, sedimentary geobiology, and implications for interpretation of outcrop rocks at Meridiani Planum, Mars. *Earth Planet Sci Lett* **240**: 149–167.  
 Fierer, N., and Jackson, R.B. (2006) The diversity and biogeography of soil bacterial communities. *Proc Natl Acad Sci USA* **103**: 626–631.  
 Garcia-Pichel, F., and Pringault, O. (2005) Cyanobacteria track water in desert soils. *Nature* **413**: 380–381.  
 González-Toril, E., Llobet-Brossa, E., Casamaior, E.O., Amann, R., and Amils, R. (2003) Microbial ecology of an

- extreme acidic environment, the Tinto river. *Appl Environ Microbiol* **69**: 4853–4865.
- Hammer, Ø., Harper, D.A.T., and Ryan, P.D. (2001) PAST: paleontological statistics software package for education and data analysis. *Palaeontol Electron* **4**: issue 1, art. 4.
- Harms (2007) Diversity of intact polar lipids in an extreme acidic environment: the Rio Tinto, Spain. Diploma Thesis. University of Bremen, Bremen, Germany.
- Hinrichs, K.-H., Summons, R.E., Orphan, V., Sylva, S.P., and Hayes, J.M. (2000) Molecular and isotopic analyses of anaerobic methane-oxidizing communities in marine sediments. *Org Geochem* **31**: 1685–1701.
- Hodkinson, I.D., Webb, N.R., and Coulson, S.J. (2002) Primary community assembly on land – the missing stages: why are the heterotrophic organisms always there first? *J Ecol* **90**: 569–577.
- Hodkinson, I.D., Coulson, S.J., and Webb, N.R. (2003) Community assembly along proglacial chronosequences in the high Arctic: vegetation and soil development in north-west Svalbard. *J Ecol* **91**: 651–663.
- Högberg, P. (1997) 15N natural abundance in soil-plant systems. *New Phytol* **137**: 179–203.
- Klingelhofer, G., Morris, R.V., Bernhardt, B., Schroder, C., Rodionov, C.S., de Souza, P.A., Jr, et al. (2004) Jarosite and hematite at Meridiani Planum from Opportunity's Mössbauer spectrometer. *Science* **306**: 1740–1745.
- Klute, A. (1986) Water retention: laboratory methods. In *Methods of Soil Analysis, Part 1: Physical and Mineralogical Methods*. Klute, A. (ed.). Madison, NJ, USA: American Society of Agronomy, Soil Science Society of America, Publisher, pp. 635–661.
- Konhauser, K. (2007) *Introduction to Geomicrobiology*. Oxford, UK: Blackwell Science.
- Lakanen, E., and Erviö, R.A. (1971) Comparison of eight extractants for the determination of plant available micro-nutrients in soils. *Suom Maataloustiet Seuran Julk* **123**: 232–233.
- Lindsay, W.L., and Norwell, W.A. (1969) Equilibrium relationship of Zn, Fe, Ca and H with EDTA and DTPA in soils. *Soil Sci Am Proc* **33**: 62–68.
- Lipp, J.S., Morono, Y., Inagaki, F., and Hinrichs, K.-U. (2008) Significant contribution of Archaea to extant biomass in marine subsurface sediments. *Nature* **454**: 991–994.
- Lizama, H.M., and Suzuki, I. (1988) Bacterial leaching of a sulfide ore by *Thiobacillus ferrooxidans* and *Thiobacillus thiooxidans*. Part I: shake flask studies. *Biotech Bioeng* **32**: 110–116.
- López, B.C., Holmgren, M., Sabaté, S., and Gracia, C.A. (2008) Estimating annual rainfall threshold for establishment of tree species in water-limited ecosystems using tree-ring data. *J Arid Environ* **72**: 602–611.
- López-Lara, I.M., Sohlenkamp, C., and Geiger, O. (2003) Membrane lipids in plant-associated bacteria: their biosyntheses and possible functions. *Mol Plant Micr Interact* **16**: 567–579.
- Nemergut, D.R., Anderson, S.P., Cleveland, C.C., Martin, A.P., Miller, A.E., Seimon, A., and Schmidt, S.K. (2007) Microbial community succession in an unvegetated, recently deglaciated soil. *Microbial Ecol* **53**: 110–122.
- Nichols, B.W., and Wood, R.J.B. (1968) New glycolipid specific to nitrogen-fixing blue-green algae. *Nature* **217**: 767–768.
- Ogle, K., and Reynolds, J.F. (2004) Plant responses to precipitation in desert ecosystems: integrating functional types, pulses, thresholds, and delays. *Oecologia* **141**: 282–294.
- Pansu, M., and Gautheyrou, J. (2006) *Handbook of Soil Analysis*. New York, NY, USA: Springer.
- Puente, M.E., Li, C.Y., and Bashan, Y. (2004a) Microbial populations and activities in the rhizoplane of rock-weathering desert plants. II. Growth promotion of cactus seedlings. *Plant Biol* **6**: 643–650.
- Puente, M.E., Li, C.Y., Bashan, Y., and Lebsky, V.K. (2004b) Microbial populations and activities in the rhizoplane of rock-weathering desert plants. I. Growth Root colonization and weathering of igneous rocks. *Plant Biol* **6**: 629–642.
- Rensing, S.A., Lang, D., Zimmer, A.D., Terry, A., Salamov, A., Shapiro, H., et al. (2008) The *Physcomitrella* genome reveals evolutionary insights into the conquest of land by plants. *Science* **319**: 64–69.
- Řezanka, T., Viden, I., Go, J.V., and Dembitzky, V.M. (2003) Polar lipids and fatty acids of three wild cyanobacterial strains of the genus *Chroococcidiopsis*. *Folia Microbiol* **48**: 781–786.
- Santi, C.A., Certini, G., and D'Acqui, L.P. (2006) Direct determination of organic carbon by dry combustion in soils with carbonates. *Comm Soil Sci Plant Anal* **37**: 155–162.
- Sasaki, K., and Konno, H. (2000) Morphology of jarosite-group compounds precipitated from biologically and chemically oxidized Fe ions. *Can Mineral* **38**: 45–56.
- Schwinning, S., Sala, O.E., Loik, M.E., and Ehleringer, J.R. (2004) Thresholds, memory, and seasonality: understanding pulse dynamics in arid/semi-arid ecosystems. *Oecologia* **141**: 191–193.
- Silverman, M.P., and Lundgren, D.G. (1959) Studies on the chemoautotrophic iron bacterium *Ferrobacillus ferrooxidans*. I. An improved medium and a harvesting procedure for securing high cell yields. *J Bacteriol* **77**: 642–647.
- Skidmore, M., Anderson, S.P., Sharp, M., Foght, J., and Lanoil, B.D. (2005) Comparison of microbial community compositions of two subglacial environments reveals a possible role for microbes in chemical weathering processes. *Appl Environ Microbiol* **71**: 6986–6997.
- Southam, G., and Beveridge, T.J. (1992) Enumeration of thiobacilli within pH-neutral and acidic mine tailings and their role in the development of secondary mineral soil. *Appl Environ Microbiol* **58**: 1904–1912.
- Sturt, H.F., Summons, R.E., Smith, K., Elvert, M., and Hinrichs, K.-U. (2004) Intact polar membrane lipids in prokaryotes and sediments deciphered by high-performance liquid chromatography/electrospray ionization multistage mass spectrometry-new biomarkers for biogeochemistry and microbial ecology. *Rapid Commun Mass Spectrom* **18**: 617–628.
- Sundareshwar, P.V., Morris, J.T., Koepfler, E.K., and Fornwalt, B. (2003) Phosphorous limitation of coastal ecosystem processes. *Science* **299**: 563–565.
- Talbot, H.M., Summons, R.E., Jahnke, L.L., Cockell, C.S., Rohmer, M., and Farrimond, P. (2008) Cyanobacterial bacteriohopanepolyol signatures from cultures and natural environmental settings. *Org Geochem* **39**: 232–263.

- Thompson, J.D., Gibson, T.J., Plewniak, F., Jeanmougin, F., and Higgins, D.G. (1997) The ClustalX windows interface: flexible strategies for multiple sequence alignment aided by quality analysis tools. *Nucleic Acids Res* **24**: 4876–4882.
- Uroz, S., Calvaruso, C., Turpault, M.P., Pierrat, J.C., Mustin, C., and Frey-Klett, P. (2007) Effects of the mycorrhizosphere on the genotypic and metabolic diversity of the bacterial communities involved in mineral weathering in a forest soil. *Appl Environ Microbiol* **73**: 3019–3027.
- Van der Wielen, P.W.J.J., Bolhuis, H., Borin, S., Daffonchio, D., Corselli, C., Giuliano, L., *et al.* (2005) The enigma of prokaryotic life in deep hypersaline anoxic basins. *Science* **307**: 121–123.
- Wang, T., and Peverly, J.H. (1998) Screening a selective chelator pair for simultaneous determination of iron (II) and iron (III). *Soil Sci Soc Am J* **62**: 611–617.
- Yoshitake, S., Uchida, M., Koizumi, H., and Nakatsubo, T. (2007) Carbon and nitrogen limitation of soil microbial respiration in a high Arctic successional glacier foreland near Ny-Ålesund, Svalbard. *Polar Res* **26**: 22–30.
- Zielke, M., Ekker, A.S., Olsen, R.A., Spjelkavik, S., and Solheim, B. (2002) The influence of abiotic factors on biological nitrogen fixation in different types of vegetation in the high arctic, Svalbard. *Arctic Antarctic Alpine Res* **34**: 293–299.

## Supporting information

Additional Supporting Information may be found in the online version of this article:

**Fig. S1.** The ML-RC1 site in the moraine of the Midtre Lovénbreen glacier, Svalbard. This site is bigger than site ML-RS1 with 10-m-long rusty leaching strip departing from a rock amphitheater. The soil crust was sampled about every 2.5 m from the origin close to the rock amphitheater to the end of the rusty colour in the grey moraine (not visible). *Acidithiobacillus ferrooxidans* most probable number counts, determined on the samples, showed decreasing values from the origin to the end (respectively,  $2.3 \times 10^4$ ,  $2.3 \times 10^3$ ,  $6.8 \times 10^2$ ,  $0.8 \times 10^1$  and  $2.3 \times 10^0$  cfu g<sup>-1</sup> wet soil).

**Fig. S2.** DRIFT spectra indicating the presence of the mineral jarosite. Relevant peaks used as signature for jarosite are indicated. a, DRIFT spectrum of the soil crust from the rusty strip of site ML-RS1. Several signature peaks of jarosite are indicated. b, DRIFT spectrum of jarosite formed by *Acidithiobacillus ferrooxidans* SB1 isolated from site ML-RS1, while growing on 9K medium containing ferrous sulfate.

**Fig. S3.** Bacterial community structure and diversity in the soil crusts of site ML-RS1. Detrended Correspondence Analysis (DCA) of the ARISA profiles obtained from all the samples withdrawn in four (A to D) minitranssects of the site. Samples were labelled with different colours according to the pH of the soil crust. Circles indicate the soil crust samples, while triangles indicate the soil withdrawn 5 cm below the soil crusts. Letters and numbers accompanying each sample, respectively, indicate the transect and the sample within the transect. Soil crust samples showed a grouping trend according to the pH, while deeper samples did not. The inset shows the correlation curve between the ARISA-based DCA axis 1 diversity index and the pH of the samples.

**Fig. S4.** Absolute ( $\mu\text{g}$  lipid/g sediment) and relative (%) lipid concentrations from transects A (A) and B (B). Sterols were not analysed in transect B. Abbreviations: heterocyst glycolipids (HG), glycosyldiacylglycerol (Gly-DAG), diglycosyldiacylglycerol (2Gly-DAG), sulfoquinovosyldiacylglycerol (SQ-DAG), glucuronic acid diacylglycerol (GlyA-DAG), phosphatidylglycerol (PG), phosphatidic acid (PA), phosphatidylserine (PS), phosphatidylinositol (PI), phosphatidylcholine (PC), phosphatidylethanolamine (PE), phosphatidyl-(N)-methylethanolamine (PME), phosphatidyl-(N,N)-dimethylethanolamine (PDME), ornithine lipids (OL) betaine lipids (BL).

**Table S1.** Fatty acid composition of IPL-glycerol derivatives. Major fatty acids found of IPL-glycerides along the two transects A and B as identified with HPLC-ESI-MS in positive and negative ion mode.

**Table S2.** Chemical, physical and microbiological parameters in the greyish, green and rusty soil crusts after removal of plant cover.

**Table S3.** Diversity indices of bacterial communities in soil crusts of site ML-RS1. Shannon–Wiener and Equitability Indices deduced from ARISA profiles and 16S rRNA gene libraries of the bacterial community in different transects within the site ML-RS1. Means  $\pm$  SD are reported.

**Table S4.** Results of the screening of 16S rRNA libraries from rusty soil crust (RUS), green soil crust (GRE) and greyish soil crust (GRY). The percentage of identified clones at phylum, class, order, and/or family and/or genus has been reported for each taxonomical rank as the average of samples of transects A and B.

Please note: Wiley-Blackwell are not responsible for the content or functionality of any supporting materials supplied by the authors. Any queries (other than missing material) should be directed to the corresponding author for the article.